Antarct. Meteorite Res., **18**, 239–252, 2005

Thermal history of chondrules during shock-wave heating

Hitoshi Miura[1,2*] and Taishi Nakamoto[3]

[1]*Graduate School of Pure and Applied Sciences, University of Tsukuba, Tsukuba 305-8577*
[2]*Research Fellow of the Japan Society for the Promotion of Science*
[3]*Center for Computational Sciences, University of Tsukuba, Tsukuba 305-8577*
[*]*Corresponding author. E-mail: miurah@ccs.tsukuba.ac.jp*

(Received August 3, 2004; Accepted December 22, 2004)

Abstract: Evaporation during chondrule melting may have resulted in depletion of volatile elements in chondrules. However, no evidence for a large degree of heavy-isotope enrichment has been reported in chondrules. In order to meet this observed constraint, the rapid heating rate at temperatures below the silicate solidus is required to form chondrules.

We have developed a new shock-wave heating model with the radiative transfer among dust particles and calculated the thermal history of chondrules. We have found that optically-thin shock waves for the thermal continuum emission from dust particles can meet the high heating rate constraint, because the dust thermal emission does not keep the dust particles high temperature for a long time in the pre-shock region and dust particles are abruptly heated by the gas drag heating in the post-shock region. We have also found a trend that the optically-thick shock waves lead to rapid heating in the pre-shock region and rapid cooling in the post-shock region. On the contrary, the optically-thin shock waves have a tendency to cause slow heating in the pre-shock region and slow cooling in the post-shock region. Since these two tendencies seem to be inconsistent with observational constraints (rapid heating and slow cooling for chondrule formation), more careful quantitative studies are needed in the future to see if the shock-wave heating model can reproduce the observations.

key words: chondrule formation, shock-wave heating, heating rate

1. Introduction

Chondrules are millimeter-sized, once-molten, spherical-shaped grains mainly composed of silicate material. They are considered to have formed from chondrule precursor dust particles about 4.5×10^9 yr ago in the solar nebula; they were heated and melted through flash heating events in the solar nebula and cooled again to solidify in a short period of time (*e.g.*, Jones *et al.*, 2000). So they must have great information on the early history of our solar system. Since it is naturally expected that protoplanetary disks around young stars in star forming regions have similar dust particles and processes, the study of chondrule formation may provide us much information on the planetary system formation. Chondrules have many features, each of which should be a clue that helps us to reveal their own formation process and that of the planetary system: physical properties (sizes, shapes, densities, degree of magnetization, etc.),

chemical properties (elemental abundances, degree of oxidation/reduction, etc.), isotopic compositions (oxygen, nitrogen, rare gases, etc.), mineralogical and petrologic features (structures, crystals, degrees of alteration, relicts, etc.), and so forth. Shock-wave heating model for chondrule formation has been studied by many authors (Hood and Horanyi, 1991, 1993; Ruzmaikina and Ip, 1994; Iida *et al*., 2001 (hereafter INSN); Desch and Connolly, 2002 (hereafter DC02); Miura *et al*., 2002; Ciesla and Hood, 2002; Miura and Nakamoto, 2005 (hereafter MN05)), and is considered to be one of the plausible mechanisms for chondrule formation (Boss, 1996; Jones *et al*., 2000).

Evaporation during chondrule melting may have resulted in depletion of volatile elements in chondrules. It is known that kinetic evaporation, especially evaporation from a melt, often leads to enrichment of heavy isotopes in an evaporation residue. However, no evidence for a large degree of heavy-isotope enrichment has been reported in chondrules. Tachibana *et al*. (2004) applied the sulfur evaporation model to the shock-wave heating conditions of MN05, and concluded that the gas drag heating in the post-shock region should be abrupt enough ($>10^4$ K/hr) so that the isotopic fractionation of sulfur is suppressed at temperatures below the silicate solidus (~1473–1573 K). As well as sulfur, there are some elements in chondrules which are not isotopically fractionated, for example, K, Fe, Mg, and Si. However, according to Tachibana and Huss (2005), these elements do not give us any information about the heating rate of chondrules because the recondensation behavior of sulfur onto chondrules would be different from that of alkali elements. During cooling, alkali elements could recondense into the silicate melt from which they evaporated. However, sulfur would not re-enter the melt because the chondrule melt would have solidified by the time sulfur began to recondense. Isotopic exchange between the sulfide veneer and the interior sulfides would be inhibited by the intervening silicate. Based on above argument, we think that the most important constraint for the heating rate of chondrules is the isotopic fractionation data of sulfur, not other element (K, Fe, Mg, and Si).

On the contrary, according to simulations of shock-wave heating by DC02, a dust particle in front of the shock front is heated by thermal radiation from dust particles, and the heating rate of the dust particles in a temperature range of 1273–1573 K is about 300 K/hr. This is so slow that the isotopic fractionation is expected to take place, which is not consistent with observations (Tachibana and Huss, 2005). Namely, if the dust temperature in the pre-shock region rises beyond 1273 K due to the thermal radiation, it is difficult to explain the isotopic fractionation data. Magnitude of the pre-shock heating due to radiation is sensitive to the optical depth in the region because the basic mechanism of this process is the blanket effect. The optical depth depends not only on the dust to gas mass ratio but also on the size distribution of the dust particles.

The purpose of this paper is to investigate how the thermal history of dust particles in the shock waves is affected by the optical properties of the pre-shock region, which depend mainly on the dust size distribution and the dust to gas mass ratio. Moreover, we attempt to confirm whether the shock-wave heating model is consistent with the isotopic fractionation data or not. In order to investigate above problems, we have developed a new shock-wave heating code with the radiative transfer among the dust particles and calculated the thermal history of chondrules. Based on our calculation results, we discuss the appropriate conditions of protoplanetary nebula in which the

isotopic fractionation is suppressed.

2. Shock-wave heating model

2.1. Dynamics and thermodynamics for gas and dusts

Basic mechanism of the shock-wave heating is rather simple. Suppose there is a gas medium containing dust particles with a dynamical equilibrium, *i.e.* they do not have a relative velocity. Suppose a shock wave passes the medium. Then, the gas is accelerated by the gas pressure and obtains some amount of velocity, while dust particles tend to remain the initial position. This causes the relative velocity between the dust particles and the gas. When the relative velocity is present, the frictional force acts and drag heating works; the intensity of the force and the heating depend mainly on the relative velocity and the gas density. Also, the high temperature gas in the post-shock region, heated by the compressional heating, heats the dust particles by thermal collisions (see Fig. 1a).

Not only in the post-shock region, but also in the pre-shock region the dust particles are heated because of the presence of radiation. Behind the shock front, there are the shocked gas and warm dust particles. The shocked gas temperature decreases by emitting line emission (mainly, from H_2O and CO). Warm dust particles are also cooled by emitting the thermal radiation. Some fraction of the line emission and the thermal continuum radiation goes toward the pre-shock region, and heats the dust particles in the region. Moreover, heated dust particles reemit their thermal radiation. The thermal radiation is absorbed by ambient other dust particles again. The more the processes continue, the stronger the radiation field becomes. This is well known as the

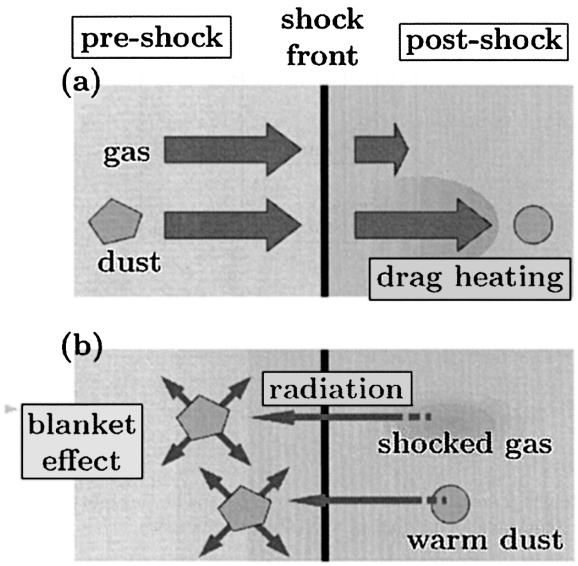

Fig. 1. Overview of shock-wave heating model: (a) gas drag heating in post-shock region and (b) radiation heating in pre-shock region.

blanket effect. By the blanket effect, dust particles are gradually heated as they go toward the shock front (see Fig. 1b).

In order to investigate the thermal history of dust particles, we have developed a new numerical model that simulates 1-dimensional plane-parallel steady shock flow including dust particles and radiative transfer. In this model, the dynamics of the gas flow and the dust particles are treated in detail. The model takes into account following physical and chemical processes: hydrodynamics of gas flow, dynamics of dust particles in the gas medium, heating/cooling of gas by several processes (compressional heating, chemical reactions, atomic/molecular radiative cooling, and interaction with dust particles), non-equilibrium chemical reactions among 32 gas species, heating/cooling of dust particles by the thermal interaction with gas and radiation, and evaporation of material from dust particles. Radiative transfer and radiative heating due to line emission from gas molecules and thermal continuum emission from dust particles will be described in Sections 2.2 and 2.3. Other details of the model are described in INSN and MN05.

It should be noted that when the flow is steady, the energy conservation equation including radiation term is given by $\rho V\ (h+1/2\ V^2)+F=$constant, where ρ is the gas density, h is the enthalpy, V is the gas velocity, and F is the *net* radiation energy flux, respectively (*e.g.*, Mihalas and Mihalas, 2000). In contrast, the jump condition which was adopted in Hood and Horanyi (1993) and DC02 (equation 3 in Hood and Horanyi, 1993 and equation 32 in DC02, respectively) for calculating the final temperature of the gas and dust particles very far from the shock front is not physically correct because σT^4 is used as the radiation term, where σ is the Stefan-Boltzmann constant and T is the gas temperature. This is not the *net* radiation energy flux. DC02 applied the incorrect jump condition to their model and obtained the final gas temperature. For example, in their nominal case ($v_s=7\,\mathrm{km\,s^{-1}}$, $\rho_1=10^{-9}\mathrm{g\,cm^{-3}}$, and $T_1=300\,\mathrm{K}$, where ρ_1 and T_1 are the pre-shock gas density and pre-shock gas temperature, respectively), the final gas temperature ends up 1143 K. On the contrary, in a physically correct view, the line emission and energy transfer between gas and dust particles cool the post-shock gas to the pre-shock gas temperature, which is namely the same as the ambient temperature surrounding the chondrule-forming region. Assuming the pre-shock temperature is 300 K, the difference between the final gas temperature of DC02 and the gas temperature in the physically correct case is about 800 K. We do not use the artificial condition for final gas temperature adopted in Hood and Connolly (1993) and DC02 and determine the gas temperature profile in the post-shock region following to basic equations for gas.

2.2. Photon escape probability method

In order to calculate the pre-shock dust temperature, we have to estimate the intensity of line emission which can escape from the post-shock region to the pre-shock region. As the gas flows further into the post-shock region, the column density between an emitting point of a fluid element and the shock front increases and it becomes difficult for the radiation to escape from the post-shock region. In INSN and MN05, this effect was taken into account approximately for the molecular vibrational emission; they evaluated the typical column density for the chondrule formation and used the spatially constant photon escape probability. On the contrary, DC02 ignored all the line

emissions from the gas. In order to clarify the importance of the gas cooling due to the line emission from gas molecules, in this study, we evaluate the photon escape probability based on results by Neufeld and Kaufman (1993), which varies with the column density, and use it when we calculate the luminosity of the gas in the post-shock region.

2.3. *Radiative transfer*

The dust particles absorb the line emissions of the gas molecules and the thermal emission of the other dust particles. These dust particles reemit the thermal radiation toward the ambient environment. As DC02 commented, the radiative transfer process may be important for the thermal history of chondrules. Thus, we take these processes into account in our model. A method of radiative transfer calculation described in DC 02 is basically used in this study. However, we add a term representing the line emission from molecules to the source function given by eq. (5) of DC02 as,

$$S=\frac{\Sigma_i 4\pi a_i^2 n_i \varepsilon_i \sigma T_i^4/(4\pi)+\Sigma_j \Lambda_j/(4\pi)}{\Sigma_i n_i \pi a_i^2 \varepsilon_i}, \tag{1}$$

where a_i, n_i, ε_i, and T_i are radius, number density, emission coefficient, and temperature of dust particles in i-th bin (see Section 2.4), respectively. We calculate the thermal history of various-sized dust particles including submicron-sized particles. So, a term corresponding to the emission from small dust particles ($<1\,\mu$m) in eq. (5) of DC02 is omitted. The cooling functions expressed by Λ_j represent the luminosity due to each line emission process, such as H_2O vibrational emission, CO vibrational emission, and so forth. We also take into account the isotropic scattering by dust particles (Rybicki and Lightman, 1979). The absorption/scattering coefficients are assumed to be the same as astrophysical silicate data (Miyake and Nakagawa, 1993).

Here, we consider 1-dimensional plane-parallel situation and take x axis perpendicularly to the shock front. We assume the calculation region is from $x=-10^5$ km to $x=10^5$ km. Outside of the computation domain is assumed to be in a thermal equilibrium with radiation from the protosun and filled with the black body radiation of 300 K, which corresponds to the temperature at 1 AU of the Minimum Mass Solar Nebula (Hayashi *et al*., 1985). Changes of the black body radiation temperature do not lead any significant change of our results shown later.

2.4. *Others*

The size distributions of dust particles in our model are shown in Fig. 2: a log-normal type and a power-law type. Regarding the dust to gas mass ratio, C_d, we assume two cases: $C_d=0.03$ and 0.10. We investigate 4 models, which are combinations of these two factors (see Table 1). In this study, we assume that the size range of dust particles is from 0.01 μm to 1 cm and divide it into 31 bins. In the shock-wave heating model, the pre-shock gas number density n_0 and shock velocity v_s are two dominant factors to determine whether the condition of the shock wave is preferable for chondrule formation or not (INSN). In this study, we examine 4 shock conditions; $(n_0, v_s)=(10^{14}\,\mathrm{cm^{-3}}, 10\,\mathrm{km\,s^{-1}})$, $(10^{13}\,\mathrm{cm^{-3}}, 22\,\mathrm{km\,s^{-1}})$, $(10^{12}\,\mathrm{cm^{-3}}, 35\,\mathrm{km\,s^{-1}})$, and $(10^{11}\,\mathrm{cm^{-3}}, 55\,\mathrm{km\,s^{-1}})$. First, we show results of $(n_0, v_s)=(10^{14}\,\mathrm{cm^{-3}}, 10\,\mathrm{km\,s^{-1}})$ and discuss in Sections 3.1, 3.2, and 3.3. In Section 3.4, we display results of other shock

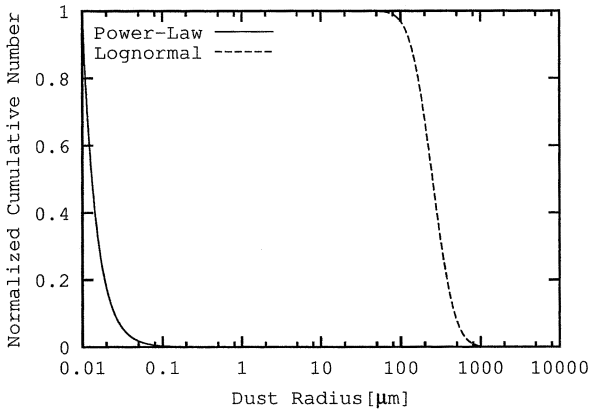

Fig. 2. Size distributions of dust particles (cumulative number of dust particles whose radii are smaller than the horizontal value) are shown as a function of dust radius. Log-normal one is assumed to be similar to measured chondrule size distribution (e.g., Nelson and Rubin, 2002).

Table 1. A list of models. There are two factors that characterize the model: the dust to gas mass ratio and the size distribution of dust particles. Size distributions are shown in Fig. 2.

		Size distribution	
		power-law	lognormal
dust/gas mass ratio	0.10	model 1	model 3
	0.03	model 2	model 4

conditions.

3. Results

3.1. Gas cooling

Figure 3 shows the gas temperature and the heating/cooling rates of gas by some major processes for model 3. The pre-shock gas number density $n_0 = 10^{14}\,\mathrm{cm}^{-3}$ and the shock velocity $v_s = 10\,\mathrm{km\,s}^{-1}$. The shock front is at $x = 0$. Behind the shock front, the gas is abruptly compressed and heated up to 4474 K. After that, its thermal energy is spent for H_2 dissociation and the gas temperature decreases to about 2000 K at $x \sim 10$ km. Then, H_2 molecules begin to increase by the three body reaction. Associating H_2 formation, the binding energy is released into the ambient environment. However, the H_2O vibrational cooling effectively removes the released energy, so the gas temperature does not increase by the H_2 formation energy. Note that we estimate the photon escape probability and reflect it to the gas cooling rate. We can see that some fraction of vibrational emissions can escape from the post-shock region.

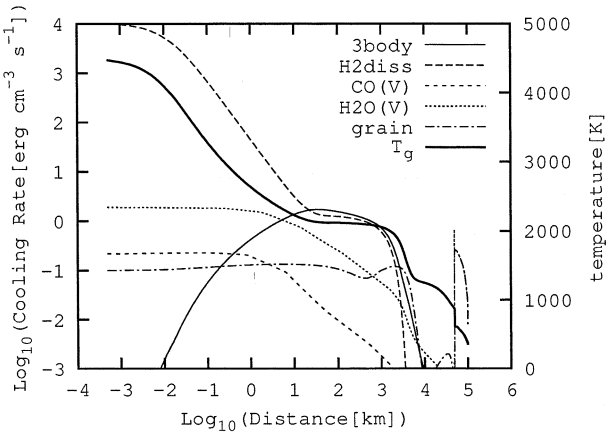

Fig. 3. Gas temperature (T_g) and heating/cooling rates of gas are plotted as a function of distance from the shock front. 3body: formation of hydrogen molecules due to 3-body reaction, H2diss: dissociation of hydrogen molecules, CO(V): CO vibrational cooling, H2O(V): H_2O vibrational cooling, grain: energy transfer between gas and dust particles due to thermal collisions.

These line emissions and dust thermal radiation in the post-shock region penetrate through the pre-shock region and heat the dust particles in the region. These dust particles reemit the thermal radiation to the circumference. Other dust particles absorb the thermal radiation and reemit their own thermal radiation. These processes are repeated more and more, and the dust particles become warmer and warmer. That is the so-called blanket effect. In the pre-shock region, the warm dust particles heat the ambient gas by means of the thermal collision.

3.2. Radiation field

In Fig. 4, we display the mean intensity (J) and temperature profiles of gas and chondrule (T_g and T_c) as functions of distance from the shock front. The shock condition is $(n_0, v_s) = (10^{14}\,\mathrm{cm}^{-3}, 10\,\mathrm{km\,s}^{-1})$. In this figure, chondrule is defined as the dust particle whose radius is 250 μm. We express the mean intensity in terms of a radiation temperature T_{rad} using an equation $T_{rad} = (\pi J/\sigma)^{1/4}$. The pre-shock gas temperatures of model 3 and 4 are not displayed in each panel because they are lower than 800 K (lower boundary of panels). We find that T_{rad} strongly depends not only on the dust to gas mass ratio but also on the dust size distribution. For the power-law size distribution (see Fig. 2), the majority of dust mass is in sub-micron sized dust particles. On the contrary, for the log-normal size distribution, most of the dust mass is in the larger (100–1000 μm) dust particles. So, even if the dust to gas mass ratio is fixed, the total surface area contributing to the opacity is larger in the power-law size distribution case than the log-normal one. Therefore, in the power-law size distribution case, the blanket effect works more effectively and T_{rad} becomes larger than the log-normal case.

We also find that T_c is almost the same as T_{rad} in the pre-shock region, so the radiation heating is the most important heating mechanism for dust particles in the

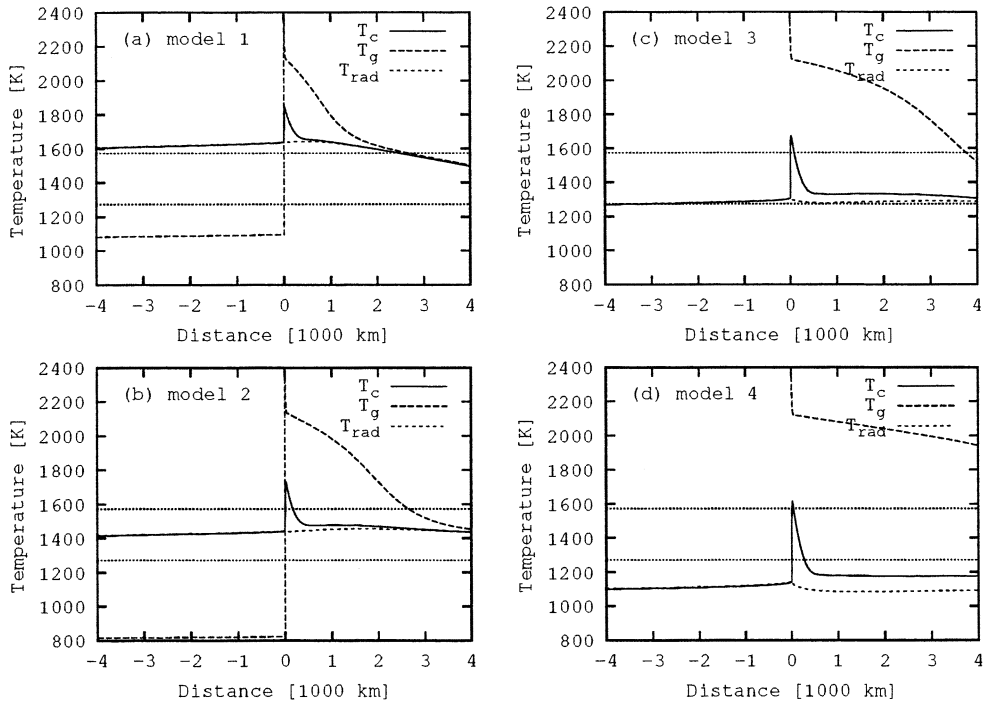

Fig. 4. Mean intensities (J) and temperatures of gas and chondrule (T_g and T_c) are plotted as functions of distance from shock front. We express the mean intensity as a radiation temperature T_{rad} using an equation $T_{rad}=(\pi J/\sigma)^{1/4}$. Two horizontal dotted lines represent 1273 K and 1573 K, respectively.

pre-shock region. These results imply that the pre-shock chondrule temperature is also strongly affected by the dust size distribution. We discuss this point further in Subsection 3.3.

3.3. Heating rate

The heating rate of the dust particles in a temperature range of 1273–1573 K is important for prevention of isotopic fractionation (Tachibana and Huss, 2005). In this study, we define the net heating rate as

$$R_{\rm heat}\equiv\frac{1573\,{\rm K}-1273\,{\rm K}}{\Delta t}, \tag{2}$$

where Δt is the difference between the time at which dust temperature reaches 1273 K and 1573 K. Figure 5 shows dust temperatures as functions of time after dust particles go through the shock front. We also calculate the heating rate and list those results in Table 2. Here, the optical depth τ is the total optical depth of the pre-shock region including absorption and scattering for near-infrared wavelengths and $T_{\rm pre}$ is the peak dust temperature in the pre-shock region, respectively. We can see that the larger the optical depth is, the lower the heating rate becomes.

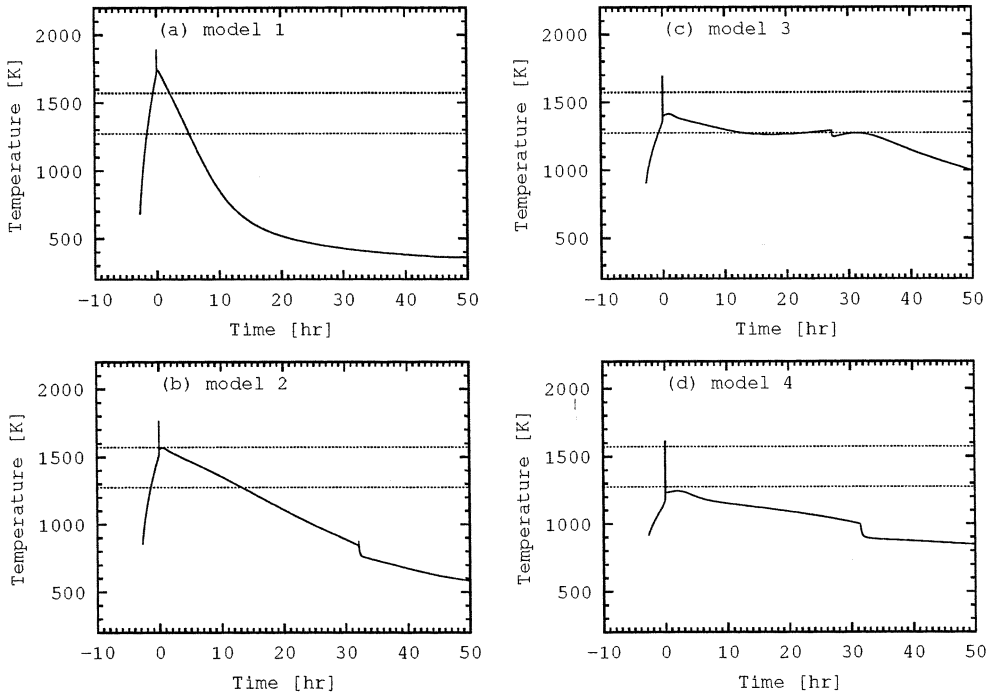

Fig. 5. Dust temperatures are plotted against time after dust particles go through shock front. Pre-shock gas number density n_0 is $10^{14} cm^{-3}$ and shock velocity v_s is $10 km\,s^{-1}$. Two horizontal dotted lines represent 1273 K and 1573 K, respectively.

Table 2. Results of pre-shock dust temperature (T_{pre}) and heating rate (R_{heat}) for each model are listed. Shock condition is (n_0, v_s) = ($10^{14} cm^{-3}$, $10 km\,s^{-1}$).

Model	τ	T_{pre} [K]	Δt [s]	R_{heat} [K/hr]
1	16.7	1635	3997	270
2	4.89	1440	3475	312
3	2.45	1304	302.5	3570
4	0.73	1211	0.904	1.19×10^6

For model 1, the blanket effect works effectively since the optical depth is large. The dust temperature increases up to 1635 K due to the radiation even if the gas drag heating does not work on them. As a result, the temperature of the dust particles are kept above 1273 K for a long time (3997 s), so the heating rate is very slow. On the contrary, for model 4, the heating rate becomes very fast because of the optically thin environment. The radiation field is too weak to heat the dust temperature above 1273 K in the pre-shock region. The dust particles are abruptly heated by the gas drag heating ($\gg 10^4$K/hr) behind the shock front, and those temperatures exceed 1573 K (silicate solids). Therefore, in model 4, chondrule formation can occur without

isotopic fractionation.

3.4. *Other shock conditions*

We showed in the previous subsections the thermal histories of chondrule in a case of $n_0 = 10^{14}\,\mathrm{cm}^{-3}$ and $v_s = 10\,\mathrm{km\,s}^{-1}$. However, Figs. 6–8 in INSN clearly indicate that chondrule formation can occur with other shock conditions. In this study, we also calculate thermal histories for other chondrule-forming shock conditions.

Based on INSN, we choose three other shock conditions; $(n_0, v_s) = (10^{13}\,\mathrm{cm}^{-3}, 22\,\mathrm{km\,s}^{-1})$, $(10^{12}\,\mathrm{cm}^{-3}, 35\,\mathrm{km\,s}^{-1})$, and $(10^{11}\,\mathrm{cm}^{-3}, 55\,\mathrm{km\,s}^{-1})$. These conditions are slightly different from the chondrule-forming condition in INSN. One of the reasons is a difference of the emission coefficient model of dust particles (for chondrule-sized particles, $\varepsilon_{em} = 0.1$ in INSN and $\varepsilon_{em} \sim 0.8$ in our model). However, basic physics of the shock-wave heating is the same except for radiation transfer.

Figures 6, 7, and 8 show the thermal histories of chondrules for $(n_0, v_s) = (10^{13}\,\mathrm{cm}^{-3}, 22\,\mathrm{km\,s}^{-1})$, $(10^{12}\,\mathrm{cm}^{-3}, 35\,\mathrm{km\,s}^{-1})$, and $(10^{11}\,\mathrm{cm}^{-3}, 55\,\mathrm{km\,s}^{-1})$, respectively. The optical depth τ, the peak dust temperature in the pre-shock region T_{pre}, the time duration Δt, and the heating rate of chondrule R_{heat} are displayed in each panel. It is found that only Fig. 6a shows slow heating ($R_{heat} \sim 10^3$ K/hr), which leads to the isotopic fractionation of sulfur. In this case, the optical depth in the pre-shock region is 1.6. On the contrary, other panels show rapid heating ($R_{heat} \sim 10^6$ K/hr), which does not cause the isotopic fractionation. In these cases, the optical depth is smaller than 0.47.

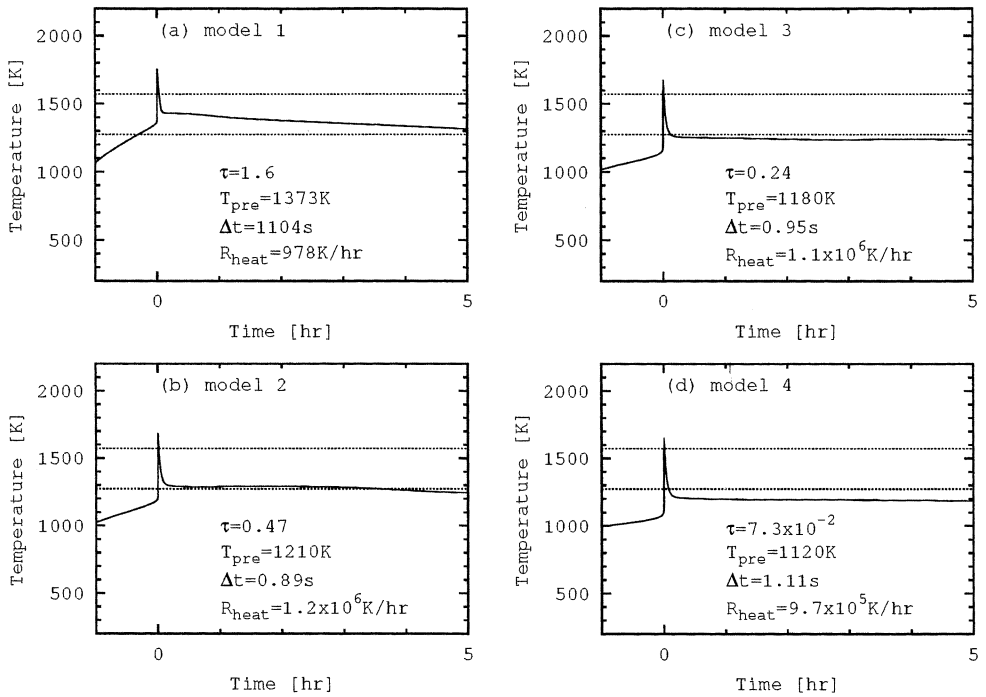

Fig. 6. Same as Fig. 5 except for $n_0 = 10^{13}\,cm^{-3}$ and $v_s = 22\,km\,s^{-1}$.

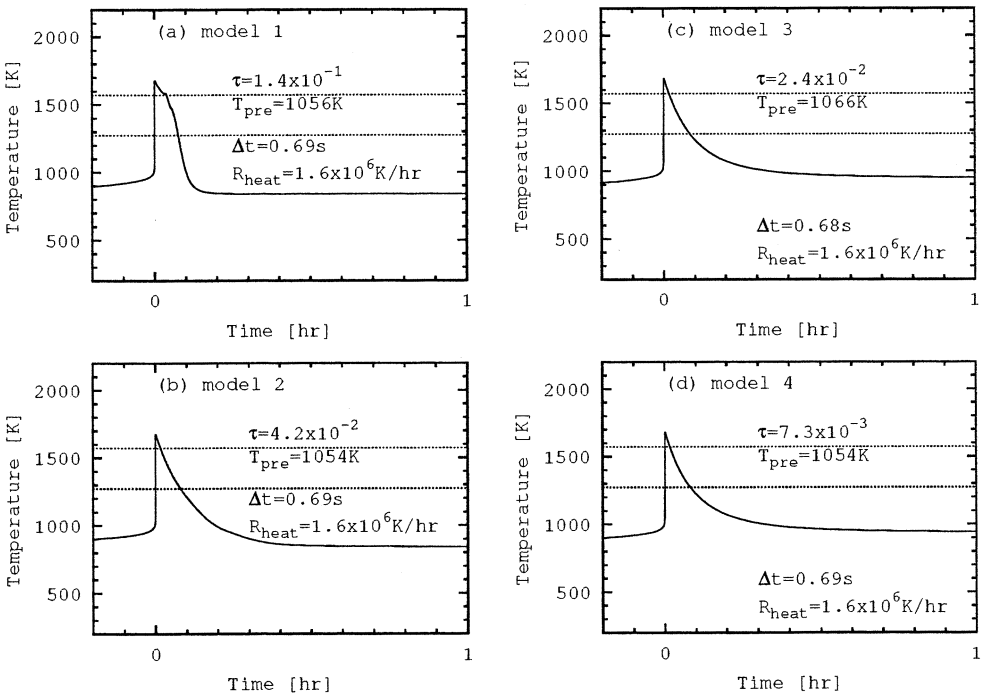

Fig. 7. Same as Fig. 5 except for $n_0=10^{12}cm^{-3}$ and $v_s=35\,km\,s^{-1}$.

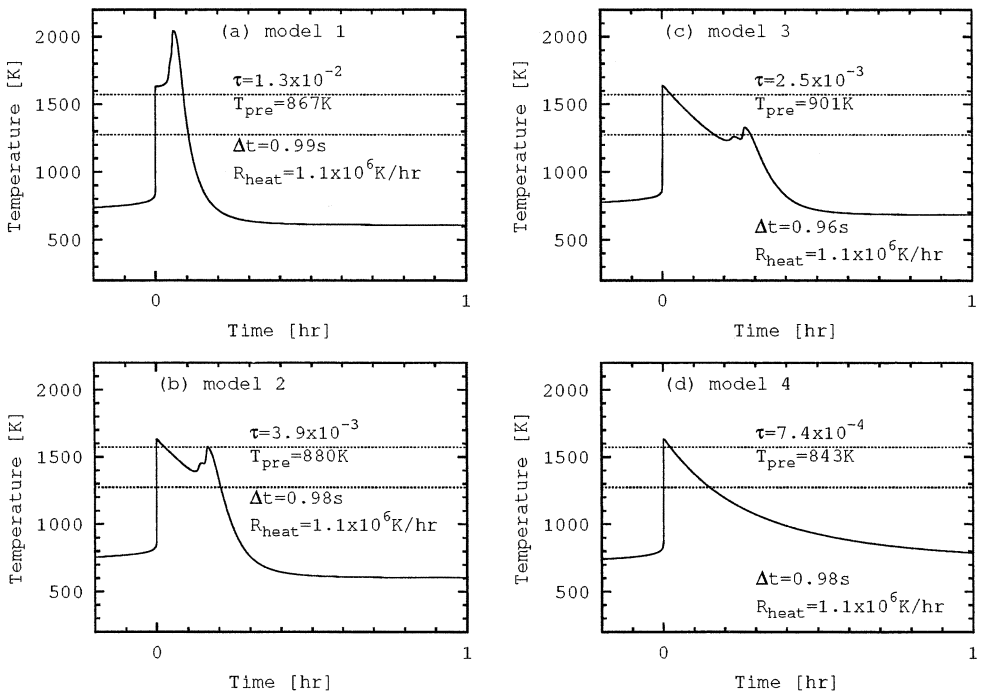

Fig. 8. Same as Fig. 5 except for $n_0=10^{11}cm^{-3}$ and $v_s=55\,km\,s^{-1}$.

Therefore, the conclusion that the optically thin environment is appropriate for rapid heating of chondrules seems to be applicable to various shock conditions.

4. Discussions

From Table 2, we can see that the size distribution of dust particles and the dust to gas mass ratio are very important factors for determination of pre-shock dust temperature and heating rate of dust particles. We also find that there is a negative correlation between the heating rate and the optical depth in the pre-shock region. In cases $\tau > 1.6$, the blanket effect works effectively in the pre-shock region and the radiation field becomes strong. The radiation field heats dust particles above 1273 K so slowly that the isotopic fractionation would occur. This is not consistent with observations (Tachibana and Huss 2005). On the contrary, in the case $\tau < 0.73$, the heating rate is very fast because the blanket effect does not work well in the pre-shock region. The dust particles are abruptly heated by the gas drag heating behind the shock front. The gas drag heating is so fast ($R_{\rm heat} \sim 10^6$ K/hr) that the isotopic fractionation is expected to be suppressed. This is consistent with observations. To summarize, shock waves in the optically thin environment can form chondrules without isotopic fractionation.

The cooling rate of chondrules in a re-solidification phase is also important for chondrule formation. The typical cooling rate is estimated roughly about 100–1000 K/hr which is indicated from experimental reproduction of chondrule textures, zoning in minerals, and presence of glass (Jones *et al*., 2000). Theoretically, some studies have discussed the cooling rates in the shock-wave heating model. For example, DC02 concluded that the cooling rates are about 50 K/hr through the crystallization temperature 1400–1730 K. Such a slow cooling rate is attributed to the radiation heating and the thermal collision with ambient hot gas in the post-shock region. Ciesla and Hood (2002) showed that the cooling rates are consistent with observations if the dust to gas mass ratio is less than about 30 times the solar abundance. If there are larger amount of dust particles, more energy of the gas would be transferred to the chondrules and then radiated away more rapidly. However, above two theoretical models did not take into account the molecular emission cooling. Since the molecular emission cooling removes the thermal energy from the post-shock gas effectively, the gas can cool more rapidly than the cases without the cooling. INSN took into consideration the molecular emission cooling in their shock calculations. INSN also assumed optically-thin shock waves for the thermal radiation from dust particles, and obtained the cooling rates 10^2–10^5 K/hr for various shock parameters. Results of INSN, obtained by the optically thin model for the thermal radiation, are consistent with estimated cooling rates, if shock waves have appropriate shock parameters.

In the present study, it has been confirmed that the strong radiation field can slow the chondrule cooling rate through the crystallization temperature range 1400–1730 K (see Fig. 4a). However, if the radiation field is so strong as to slow the chondrule cooling rate, the isotopic fractionation would take place due to the strong radiation heating in the pre-shock region. As seen in Figs. 5–8, there is a trend that rapid cooling is followed on rapid heating and slow cooling is followed on slow heating. Since the slow cooling is appropriate for chondrule formation, a flow with the strong radiation

field may not reconcile the chondrule cooling rate constraint and the pre-shock heating constraint successfully. This problem should be argued in more detail in the future.

5. Conclusion

We conclude that the shock-wave heating model is consistent with isotopic fractionation data if the flow is optically thin for the thermal radiation from dust particles. Moreover, there is a trend that rapid cooling is followed on rapid heating and slow cooling is followed on slow heating. We would now like to go on to develop our study by investigating the relation of heating rate in the pre-shock region to cooling rate in the post-shock region carefully.

Acknowledgments

We are grateful to S. Tachibana for useful discussion on observations of isotopic fractionation and pre-shock heating rates. HM was supported by the Research Fellowship of Japan Society for the Promotion of Science for Young Scientists. TN was supported by Grant-in-Aid for Young Scientists (B) (14740284) of Japan Society for the Promotion of Science.

References

Boss, A.P. (1996): A concise guide to chondrule formation models. Chondrules and the Protoplanetary Disk, ed. by R.H. Hewins *et al*. Cambridge, Cambridge Univ. Press, 257–263.

Ciesla, F.J. and Hood, L.L. (2002): The nebular shock wave model for chondrule formation: Shock processing in a particle-gas suspension. Icarus, **158**, 281–293.

Desch, S.J. and Connolly, H.C., Jr. (2002): A model of the thermal processing of particles in solar nebula shocks: Application to the cooling rates of chondrules. Meteorit. Planet. Sci., **37**, 183–207 (DC02).

Hayashi, C., Nakazawa, K. and Nakagawa, Y. (1985): Formation of the solar system. Protostars and Planets II, ed. by D.C. Black and M.S. Matthews. Tucson, Univ. Arizona Press, 1100–1153.

Hood, L.L. and Horanyi, M. (1991): Gas dynamic heating of chondrule precursor grains in the solar nebula. Icarus, **93**, 259–269.

Hood, L.L. and Horanyi, M. (1993): The nebular shock wave model for chondrule formation: One-dimensional calculations. Icarus, **106**, 179–189.

Iida, A., Nakamoto, T., Susa, H. and Nakagawa, Y. (2001): A shock heating model for chondrule formation in a protoplanetary disk. Icarus, **153**, 430–450 (INSN).

Jones, R.H., Lee, T., Connolly, H.C., Jr., Love, S.G. and Shang, H. (2000): Formation of chondrules and CAIs: Theory vs. observation. Protostars and Planet IV, ed. by V. Mannings *et al*. Tucson, Univ. Arizona Press, 927–961.

Mihalas, D. and Mihalas, B. (2000): Foundations of Radiation Hydrodynamics. New York, Dover Publications, Inc. 916 p.

Miura, H. and Nakamoto, T. (2005): A shock-wave heating model for chondrule formation. II. Minimum size of chondrule precursors. Icarus (in press) (MN05).

Miura, H., Nakamoto, T. and Susa, H. (2002): A shock-wave heating model for chondrule formation: Effects of evaporation and gas flows on silicate particles. Icarus, **160**, 258–270.

Miyake, K. and Nakagawa, Y. (1993): Effects of particle size distribution on opacity curves of protoplanetary disks around T Tauri stars. Icarus, **106**, 20–41.

Nelson, V.E. and Rubin, A.E. (2002): Size-frequency distributions of chondrules and chondrule fragments in LL3 chondrites: Implications for parent-body fragmentation of chondrules. Meteorit. Planet. Sci.,

37, 1361–1376.
Neufeld, D.A. and Kaufman, M.J. (1993): Radiative cooling of warm molecular gas. Astrophys. J., **418**, 263–272.
Ruzmaikina, T.V. and Ip, W.H. (1994): Chondrule formation in radiative shock. Icarus, **112**, 430–447.
Rybicki, G.B. and Lightman, A.P. (1979). Radiative Processes in Astrophysics. New York, John Wiley, 382 p.
Tachibana, S. and Huss, G.R. (2005): Sulfur isotopic composition of putative primary troilite in chondrules from Bishunpur and Semarkona. Geochim. Cosmochim. Acta (in press).
Tachibana, S., Huss, G.R., Miura, H. and Nakamoto, T. (2004): Evaporation and accompanying isotopic fractionation of sulfur from Fe-S melt during shock wave heating. Lunar and Planetary Science XXXV. Houston, Lunar Planet. Inst., Abstract #1549 (CD-ROM).